



AIAS 2019 International Conference on Stress Analysis

## Analysis of the micro-voids fraction in structural steels and its evolution during plastic deformation until failure

Francesco Iob<sup>a\*</sup>, Luca Cortese<sup>b</sup>, Andrea Di Schino<sup>c</sup>, Tommaso Coppola<sup>a</sup>

<sup>a</sup>*Rina Consulting – Centro Sviluppo Materiali S.p.A, Via di Catsel Romano 100, 00128 Roma, Italy.*

<sup>b</sup>*Department of Mechanical and Aerospace Engineering, Sapienza University of Rome, Via Eudossiana 18, 00184 Roma, Italy.*

<sup>c</sup>*Department of Engineering, University of Perugia, 06125 Perugia, Italy.*

---

### Abstract

In this work the results of an experimental analysis performed on different steels of commercial use having different microstructure and yield value are reported. The materials were characterized by performing tensile and torsion tests, bringing the material up to rupture. The specimens were extracted according to different orientations to verify the influence of anisotropy on the size and distribution of micro-voids present in the broken material. After the mechanical tests, an analysis was made of the amount of micro-voids present in the original, not deformed material and in the deformed material until failure. The results obtained show that for all the analyzed steels the initial fraction of micro-voids is negligible, and no growth or formation of further voids is observed as the applied plastic deformation increases, even for strain values close to rupture.

© 2019 The Authors. Published by Elsevier B.V.

This is an open access article under the CC BY-NC-ND license (<http://creativecommons.org/licenses/by-nc-nd/4.0/>)

Peer-review under responsibility of the AIAS2019 organizers

*Keywords:* mechanics; microstructure; fracture; anisotropy

---

### 1. Introduction

The ductile fracture in metal alloys like steels is usually described as a progressive damaging mechanism based on the void nucleation from defects like inclusions and their coalescence up to the inter-void ligaments fracture. Based on this, many fracture criteria have been proposed based on void evolution theories (McClintock, 1968, Rice, 1969). The matrix softening has been also described by porous models, the most popular one being the GTN (Gurson, 1977, Tvergaard, (1984)). Moreover, to identify the material parameters for this class of models, alternative experimental measurements of stiffness reduction in tensile strained specimens have been proposed to describe the matrix degradation. (Lemaitre (1985)). As a consequence, the damage evolution is then coupled to the plasticity, and the material constitutive law is modified by the introduction of the softening, which progressively degrades the yield surface. In this paper experimental observation on strained and fractured specimens under different stress states was reported. Moreover, it is well known that steel chemical composition and cooling processes are the most significant parameters affecting micro-structure (Suikkanen et al. (2008), Di Schino et al. (2007), Mengaroni et al. (2015), Rufini et al. (2018). Therefore,

---

\* Corresponding author. Tel.: +39-06-5055745.

E-mail address: [francesco.iob@rina.org](mailto:francesco.iob@rina.org)

materials are selected from commercial steels for automotive or pipeline applications, in different grades, microstructures and delivery conditions (annealed, cold worked, heat treated).

The mechanical characterization is based on tensile tests with smooth cylindrical geometry and torsion tests.

Subsequently to mechanical tests fracture surfaces and section of selected specimen were analyzed by Electronic Microscope (SEM) for voids and inclusions counting. Void counting was carried out on virgin material and on areas next to the fracture surface where the material reach elevated strain values.

## 2. Materials and Methods

A number of steel grades has been selected and characterized by means of tensile and torsion mechanical tests (Coppola et al. (2014), Iob et al. (2019)). The complete list of materials is reported in the subsequent Table 1.

Table 1. Materials with delivery state

Steel grade	Product form	Delivery state	Processing route
33MnB5	Seamless pipe	Annealed	Piercing , rolling, cold drawing
33MnB5	Seamless pipe	Quenched and Relieved	Piercing , rolling, cold drawing
20MnCrS4	Seamless pipe	As drawn	Piercing , rolling, cold drawing
20MnCrS4	Seamless pipe	Annealed	Piercing , rolling, cold drawing
25MnCrS6	Seamless pipe	Normalized	Piercing , rolling, cold drawing
25MnCrS6	Seamless pipe	Quenched and Relieved	Piercing , rolling, cold drawing
X52	Seamless pipe	Normalized	Piercing , rolling
X70	UOE pipe	As formed	TMCP plate rolling, UOE forming
X80	UOE pipe	As formed	TMCP plate rolling, UOE forming
X70	Spiral pipe	As formed	TMCP coil rolling, Spiral forming

For all materials the specimen for mechanical test are extracted in the longitudinal direction of the pipes. However, for the X70 spiral pipe, the material anisotropy was characterized by tensile and torsion tests carried out in the base material of the pipe with tensile specimen extracted in different orientations. Three standard tensile tests, with geometry according to UNI EN ISO 6892-1:2009 are carried out on round bar smooth specimens having 9 mm gauge section diameter, extracted in the longitudinal (L), transversal (T) and at 45 ° degrees between L-T directions (45 °LT) of the pipe.

Torsion tests were also performed in the longitudinal (L) and transversal direction (T) on round bar specimens having a gauge diameter of 8 mm and a gauge length of 17 mm (Fig. 1).

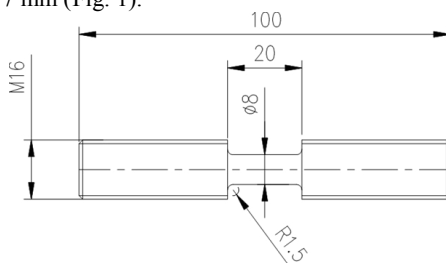


Fig. 1. Torsion specimen

A custom tension-torsion equipment has been used, capable of maximum axial and torsional loads of 100kN and 1000 Nm, axial stroke up to 150 mm and unlimited rotation angle. Torque and rotation are measured by means of a biaxial load cell and a digital encoder. All tests have been executed in a free-end configuration (null axial load) to ensure a pure shear state of stress.

## 3. Results

The micrographic examination was performed on smooth tensile and torsion specimens. For each material, SEM documentation of fractured surface to analyze and quantify the dimple pattern was performed, next specimens were sectioned along a radial plane to analyze the longitudinal section, followed by polishing for the voids and inclusions characterization. Void counting was extended to areas taken along the longitudinal specimen axis starting from the fractured surface (Fig. 2).

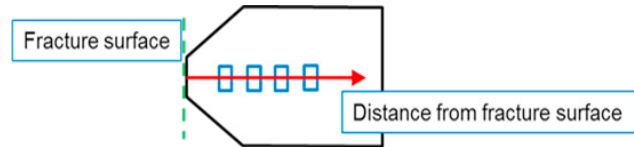


Fig. 2. Void counting procedure

Results of the voids counting are reported in the following Table 2 for all the materials excluding the X70 spiral pipe for which a more extensive results are reported in the subsequent paragraphs.

Table 2. Voids fractions

Steel grade	Delivery state	Test	Voids fraction (%) at fracture	Voids fraction (%) 2mm from fracture	Voids fraction (%) undeformed
33MnB5	Annealed	Tensile	0.062	0.198	0.085
33MnB5	Annealed	Torsion	0.049	0.033	0.085
33MnB5	Quenched and Relieved	Tensile	0.175	0.034	0.039
33MnB5	Quenched and Relieved	Torsion	0.008	0.061	0.032
20MnCrS4	As drawn	Tensile	0.462	0.212	0.143
20MnCrS4	As drawn	Torsion	0.018	0.157	0.540
20MnCrS4	Annealed	Tensile	0.317	0.072	0.027
20MnCrS4	Annealed	Torsion	0.555	0.228	0.088
25MnCrS6	Normalized	Tensile	0.057	0.030	0.014
25MnCrS6	Normalized	Torsion	0.041	0.072	0.000
25MnCrS6	Quenched and Relieved	Tensile	0.0874	0.116	0.511
25MnCrS6	Quenched and Relieved	Torsion	0.017	0.041	0.032
X52	Normalized	Tensile	0.001	0.000	0.000
X52	Normalized	Torsion	0.002	0.002	0.003
X70	As formed	Tensile	0.038	0.001	0.013
X70	As formed	Torsion	0.004	0.014	0.002
X80	As formed	Tensile	0.001	0.001	0.001

### 3.1. Fractographic analysis results

The X70 spiral pipe material has been characterized, quantifying the void distribution on virgin materials and on deformed and fractured tensile specimens extracted in the longitudinal (L), transversal (T) and 45 ° degrees between L-T directions (45 °LT) of the pipe. For each specimen, SEM documentation of fractured surface to analyze and quantify the dimple pattern was performed (Fig. 3 to Fig. 5).

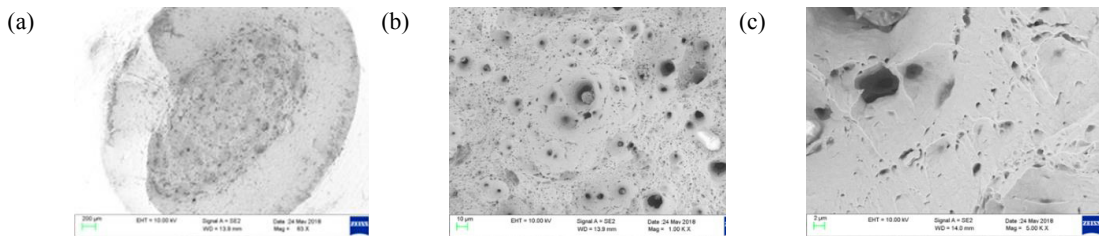


Fig. 3. SEM Analysis of X70 Transversal pipe tensile specimen: (a) Mag 63 X; (b) Mag 1000 X; (c) Mag 5000 X.

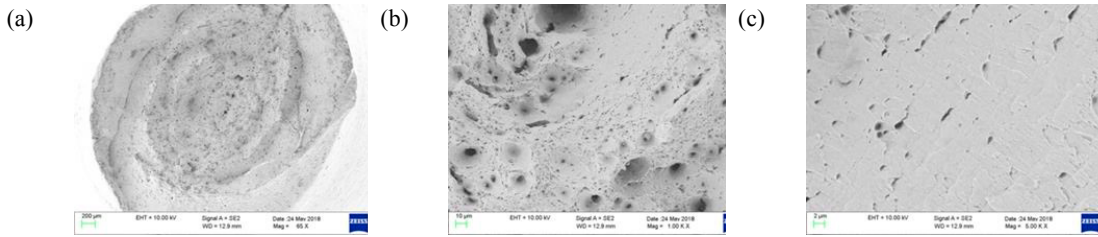


Fig. 4. SEM Analysis of X70 Longitudinal pipe tensile specimen: (a) Mag 63 X; (b) Mag 1000 X; (c) Mag 5000 X.

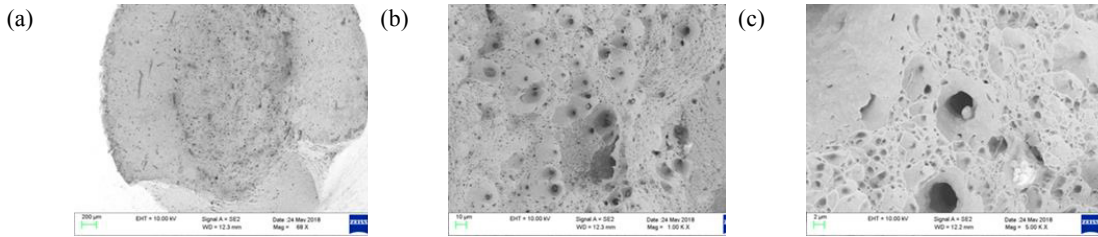


Fig. 5. SEM Analysis of X70 45° LT pipe tensile specimen: (a) Mag 63 X; (b) Mag 1000 X; (c) Mag 5000 X.

### 3.2. Material voids count

After the tests the specimens were sectioned along a radial plane to analyze the longitudinal section, followed by polishing for the voids and inclusions characterization. Selected specimens were sectioned and analyzed for voids and inclusions counting on a remote area from fractured surface to assess the void fraction on virgin material. Next void counting was extended to areas taken along the longitudinal specimen axis starting from the fractured surface.

The void counting results for the X70 spiral pipe material are reported in the following Fig. 6, Fig. 7

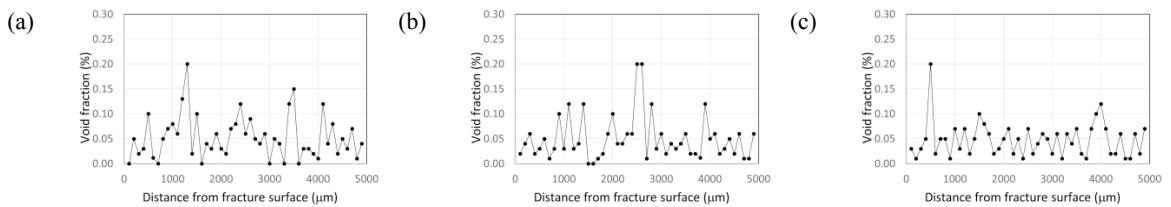


Fig. 6. Void counting performed on tensile specimens after the test: (a) Transversal pipe tensile specimen; (b) Longitudinal pipe tensile specimen; (c) 45° LT pipe tensile specimen.

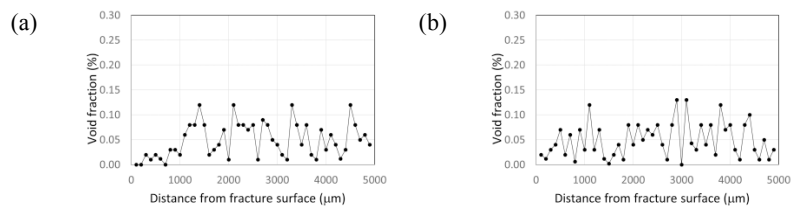


Fig. 7. Void counting performed on torsion specimens after the test: (a) Transversal pipe tensile specimen; (b) Longitudinal pipe tensile specimen.

## 4. Conclusions

The results described above show that in modern steels the measured void fraction is fully negligible even at the fracture proximity. Voids fractions are unrelated to the plastic strain reached from the material, and to the material orientation. Even if the ductile fracture is governed by the evolution (nucleation, growth and coalescence) of existing defects (initial voids and inclusions) it is not possible to find a clear correlation between the amount of plastic strain cumulated in the tensile specimens and the area fraction of defects. Moreover, no clear differences have been observed for the dimple geometries of the three tensile specimens oriented in different directions. Geometry of the dimples on the fracture surfaces is almost circular, even though the cross sectional area of the specimens presented an elliptical geometry due to the anisotropic behavior of the material. Therefore, damage evolution

seems not governed by microvoids evolution and the plastic damage mechanism is different from the classical one based on voids evolution. Furthermore, the global anisotropic behavior of the material seems to not affect locally the fracture surface aspect.

This could justify a different approach to the problem of modelling the plastic deformation and damage of these alloy steels. The damage evolution could be regarded as uncoupled from the plastic behavior, and even if an anisotropic plasticity criterion is needed to correctly describe the material, the damage model could be even based on a simple isotropic formulation as a first attempt.

## References

- Coppola, T., Iob, F., Campanelli, F., 2014 Critical review of ductile fracture criteria for steels, 20th European Conference on Fracture (ECF20), Steel Rolling, Proceedings, Norway.
- Di Schino, A.; Porcu, G.; Longobardo, M.; Turconi, G.; Scoppio, L., 2006, Metallurgical design and development of C125 grade for mild sour service application. In NACE- International Conference Series, San Diego, CA, USA, 2006; pp. 06125-0612514.
- Gurson A.L (1977). Continuum theory of ductile rupture by void nucleation and growth. Part I. Yield criteria and flow rules for porous ductile media. *J. Eng. Mater. Tech.* 99, 2–15.
- Iob, F., Coppola, T., Di Schino, A., 2019, Analysis of anisotropic hardening in high strength steel in linepipes for strain-based applications, *Metalurgija*, 58, 95-98.
- Iob, F., Cortese, L., Di Schino, A., Coppola, T., 2019, Influence of Mechanical Anisotropy on Micro-Voids and Ductile Fracture Onset and Evolution in High-Strength Low Alloyed Steels. *Metals*, 9, 224.
- McClintock, F. A., 1968, A criterion for ductile fracture by growth of holes. *J Appl Mech- T ASME* 35:363–371.
- Mengaroni, S., Cianetti, F., Calderini, M., Evangelista, E., Di Schino, A., McQueen, H., 2015, Tool steels: forging simulation and microstructure evolution of large scale ingot. *Acta Physica Polonica*, 128, 629-632.
- Rice J.R., Tracey D.M., 1969, On the ductile enlargement of voids in triaxial stress fields. *J Mech Phys Solids* 17, 201–217.
- Rufini, R., Di Pietro, O., Di Schino, A., 2018, Predictive simulation of plastic processing of welded stainless steel pipes. *Metals*, 8, 519.
- Suikkanen, P., Karjalainen, L., DeArdo, A., 2008, Effect of carbon content on the phase transformation characteristics, microstructure and properties of 500 MPa grade microalloyed steels with non-polygonal ferrite microstructures. *La Metallurgia Italiana*, 6, 41–54
- Tvergaard, V., Needleman, A., 1984, Analysis of the cup-cone fracture in a Round Tensile Bar. *Acta Metall.*, 32, 157-169.